

# Optical Flow Estimation of a Fluid Based on a Physical Model

Jin-Woo Kim, Member, KIMICS

**Abstract**—An estimation of 3D velocity field including occluded parts without maxing tracer to the fluid had not only never been proposed but also impossible by the conventional computer vision algorithm. In this paper, we propose a new method of three dimensional optical flow of the fluid based on physical model, where some boundary conditions are given from a priori knowledge of the flow configuration. Optical flow is obtained by minimizing the mean square errors of a basic constraint and the matching error terms with visual data using Euler equations. Here, Navier-Stokes motion equations and the differences between occluded data and observable data are employed as the basic constrains. we verify the effectiveness of our proposed method by applying our algorithm to simulated data with partly artificially deleted and recovering the lacking data. Next, applying our method to the fluid of observable surface data and the knowledge of boundary conditions, we demonstrate that 3D optical flow are obtained by proposed algorithm.

**Index Terms**—Optical flow, Naver-Stokes equation, Fluid flow, Regularization.

## I. INTRODUCTION

IN fluid engineering, measuring of velocity field are carried out by numerical method or by some device instruments conventionally[1]~[4]. Estimation by image processing approach has a feature of noncontact with the flow. An optical flow is the apparent two dimensional velocity field obtained from two sequential images, in which the corresponding points are searched in some ways. Obtaining the velocity of rigid or deformable object may be easier than that of

fluid. There are two major approaches to obtaining optical flow. One is the correlation method, and the other is the gradient method [5][6]. In the gradient method, a smoothness constraint is introduced to avoid the aperture problem, because the flow vectors are not determined uniquely without using some kinds of regularization as imposing spacial smoothness constraint to the flow vector field. The optical flow algorithm proposed by Horn & Shanck [5][6] is very effective and so many researches are followed and developed in various ways. However, the smoothness constraint has no strong bases but is only heuristics. Thus, it will be reasonable to use a physical model for the regularization or other kind of techniques to determine the solution uniquely when we know the characteristics of the object. Physical models were used such as for determining three dimensional motion of deformable objects from marker points on a object [7] and of lattice points of a spring model of faces [8], where motion equations were employed. In contrast to these in this paper, we propose 3D optical flow of the fluid using top surface image, where some boundary conditions are given from the surface image and a priori knowledge of the flow configuration is also given. It is well known that the physics of the fluid is given by Navier-Stokes equation (NSE). In this paper, we apply it to 3D case using the NSE for the regularization of the optical flow instead of the energy function; i.e., minimization of square errors.

## II. FLUID EQUATION

In this paper, we deal with incompressible viscous fluid with constant density spacially and temporarily. The basic equations of the fluid are continuous equation and NSE. The continuous equation is 3D tubular structure (line) orthogonal to the xy-plane is modeled as

$$\frac{\partial U}{\partial X} + \frac{\partial V}{\partial Y} + \frac{\partial W}{\partial Z} = 0 \quad (1)$$

and the motion equation is

Manuscript received November 5, 2009 ; revised November 24, 2009.

Jin-Woo Kim is with the Department of Multimedia and Communication Engineering , Kyungsung University, Busan, 314-79, Korea (Tel: +82-51-663-5153, Fax: +82-51-625-1402, Email: jinwoo@ks.ac.kr)

$$\begin{aligned} \frac{\partial U}{\partial t} + U \frac{\partial U}{\partial X} + V \frac{\partial U}{\partial Y} + W \frac{\partial U}{\partial Z} + \frac{1}{\rho} \frac{\partial P}{\partial X} \\ - gx - \nu \nabla^2 U = 0 \end{aligned} \quad (2)$$

$$\begin{aligned} \frac{\partial V}{\partial t} + U \frac{\partial V}{\partial X} + V \frac{\partial V}{\partial Y} + W \frac{\partial V}{\partial Z} + \frac{1}{\rho} \frac{\partial P}{\partial Y} \\ - gy - \nu \nabla^2 V = 0 \end{aligned} \quad (3)$$

$$\begin{aligned} \frac{\partial W}{\partial t} + U \frac{\partial W}{\partial X} + V \frac{\partial W}{\partial Y} + W \frac{\partial W}{\partial Z} + \frac{1}{\rho} \frac{\partial P}{\partial Z} \\ - gz - \nu \nabla^2 W = 0 \end{aligned} \quad (4)$$

where  $U, V, W$  are velocity components along  $X, Y, Z$  axes, respectively,  $P$  is pressure,  $t$  is time,  $\rho$  is density,  $\nu$  is kinetic viscosity,  $g_x, g_y, g_z$  are gravity components along the corresponding  $X, Y, Z$  axes, respectively.

### III. EVALUATION FUNCTION

In addition to use fitness constraint of the measured image data obtained sequentially, we define an evaluation function using two constraint equations of continuity and the NSE. The first constraint of the equation of continuous is

$$e_c = (U_x + U_y + U_z)^2 \quad (5)$$

where  $U_x = \frac{\partial U}{\partial X}, V_y = \frac{\partial V}{\partial Y}, W_z = \frac{\partial W}{\partial Z}$ . Second one of the motion equation is

$$e_M = (NSE_{(U)})^2 + (NSE_{(V)})^2 + (NSE_{(W)})^2 \quad (6)$$

and the third one by the measured image data is

$$\begin{aligned} e_D = \alpha_U (U - U_{data})^2 + \alpha_V (V - V_{data})^2 \\ + \alpha_W (W - W_{data})^2 \end{aligned} \quad (7)$$

where  $NSE_{(U)}, (V), (W)$  are equations of motion (Eq.(2) ~ (4)),  $U_{data}, V_{data}, W_{data}$  are measured data existed ( $\alpha_{U,V,W} = 1$ ) or not ( $\alpha_{U,V,W} = 0$ ). Thus, we define the total evaluation function

$$E = e_c + \lambda_1 e_M + \lambda_2 e_D \quad (8)$$

where,  $\lambda_1, \lambda_2$  are weighting coefficients. Mathematically, they are known as Lagrange's coefficients. We determined their values experimentally.

### IV. ANALYSIS

The evaluation function over the region of interest is defined by

$$\begin{aligned} \iiint E(U, V, W, U_x, U_y, U_z, V_x, V_y, V_z, \\ W_x, W_y, W_z, P_x, P_y, P_z, U_{xx}, U_{yy}, U_{zz}, \\ V_{xx}, V_{yy}, V_{zz}, W_{xx}, W_{yy}, W_{zz}) dXdYdZ \end{aligned} \quad (9)$$

where the notations of  $U_x$  means partial differentiation of  $U$  by  $X$  and  $U_{xx}$  means partial differentiation of  $U_x$  by  $X$ . Another notations are defined by the same manner. The solution of minimizing this type of integral is given by the following Euler equation :

$$\begin{aligned} E_U - \frac{\partial E_{U_x}}{\partial X} - \frac{\partial E_{U_y}}{\partial Y} - \frac{\partial E_{U_z}}{\partial Z} + \frac{\partial^2 E_{U_{xx}}}{\partial X^2} \\ + \frac{\partial^2 E_{U_{yy}}}{\partial Y^2} + \frac{\partial^2 E_{U_{zz}}}{\partial Z^2} = 0 \end{aligned} \quad (10)$$

$$\begin{aligned} E_V - \frac{\partial E_{V_x}}{\partial X} - \frac{\partial E_{V_y}}{\partial Y} - \frac{\partial E_{V_z}}{\partial Z} + \frac{\partial^2 E_{V_{xx}}}{\partial X^2} \\ + \frac{\partial^2 E_{V_{yy}}}{\partial Y^2} + \frac{\partial^2 E_{V_{zz}}}{\partial Z^2} = 0 \end{aligned} \quad (11)$$

$$\begin{aligned} E_W - \frac{\partial E_{W_x}}{\partial X} - \frac{\partial E_{W_y}}{\partial Y} - \frac{\partial E_{W_z}}{\partial Z} + \frac{\partial^2 E_{W_{xx}}}{\partial X^2} \\ + \frac{\partial^2 E_{W_{yy}}}{\partial Y^2} + \frac{\partial^2 E_{W_{zz}}}{\partial Z^2} = 0 \end{aligned} \quad (12)$$

$$\begin{aligned} \frac{\partial E_{P_x}}{\partial X} - \frac{\partial E_{P_y}}{\partial Y} - \frac{\partial E_{P_z}}{\partial Z} = 0 \end{aligned} \quad (13)$$

We solve these nonlinear simultaneous differential equations by the Newton-Rapson method.

**V. SIMULATION AND RESULTS**

The flow configuration used for simulation is shown in Fig. 1, where the bottom is wall and the top surface is free and the left side bottom surface has a step-like change.

Boundary condition of the top surface is free flow with no wall. The viscosity is made uniform independent of positions and time in the following all simulations.

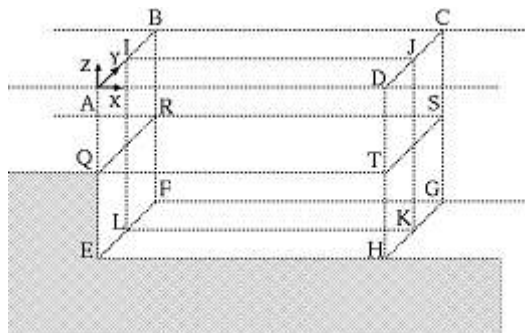
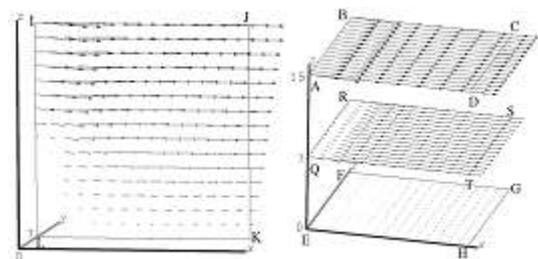


Fig.1 Definition of simulation field.

**A. Simulated flow**

First, we expand the Euler eq. and NSE to numerical equations by using software program Mathematica. We used a flow line vortex method for generating the simulated flow. Here, the pressure term including ambiguity is changed to stream function and disappears in the equations.

We define some horizontal and vertical flow planes as shown in Fig. 2. The size of numerical simulation field  $[X \times Y \times Z]$  is  $16 \times 16 \times 16$ . Fig. 2 shows a simulated flow. The initial and boundary condition for the velocity components are assigned to zero on the base plane  $[EFGH]$  and side plane  $[QRFE]$ , which correspond to shaded regions in Fig. 1.



(a)vertical plane (b)horizontal plane

Fig. 2 Simulated true flow.

**B. Recovery of lacking data cases**

When the velocity data are lacking at shaded portion of case 1~3, we recover the flow by the proposed algorithm.

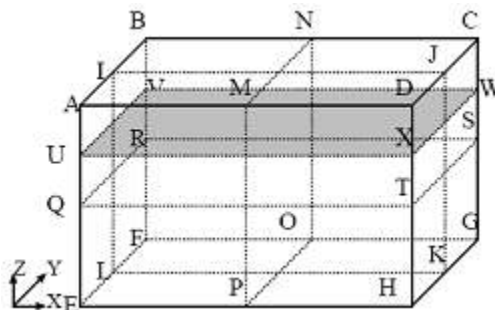
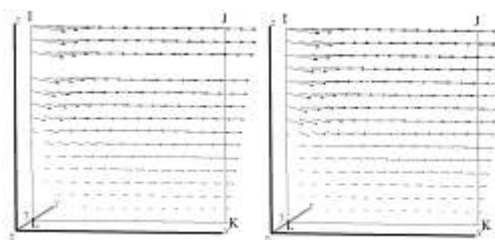
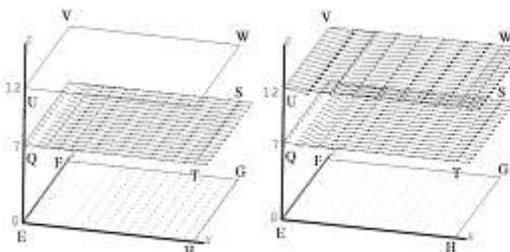


Fig. 3 case 1: All data are made lacking in a shaded plane.

[case 1] Set the velocity data zero(lacking) on a X-Y horizontal plane  $(Z=12)$ . The shaded portion of Fig. 3 is area of set zero. The recovered results are shown in Fig. 4.



(a)Initial flow (b)converged flow (A)vertical plane



(a)Initial flow (b)converged flow (B)horizontal plane

Fig. 4 Recovered flow of Fig.3(case 1).

[case 2] Set the velocity data zero (lacking) on a Y-Z vertical plane  $(X=10)$ . The shaded portion of Fig. 5 is area of set zero. The recovered results are shown in Fig.6.

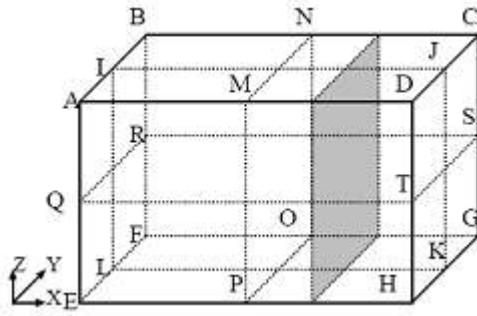
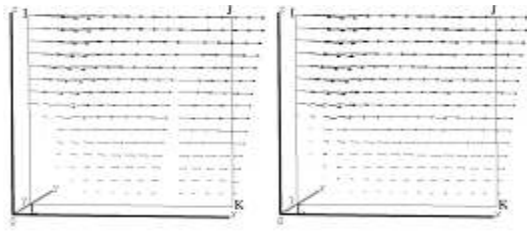
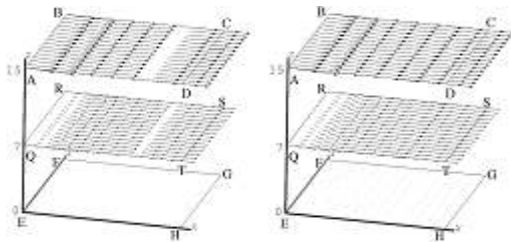


Fig. 5 case 2: All data are made lacking in a shaded plane.



(a)Initial flow (b)converged flow  
(A)vertical plane



(a)Initial flow (b)converged flow  
(B)horizontal plane

Fig. 6 Recovered flow of Fig.5(case 2).

[case 3] Set the velocity data zero (75% lacking) on Y-Z vertical planes ( $X=4-15$ ). The shaded portion of Fig. 7 is area of set zero. The recovered results are shown in Fig. 8.

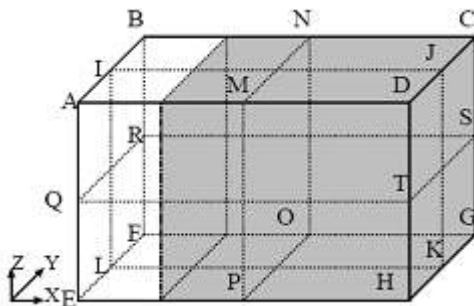
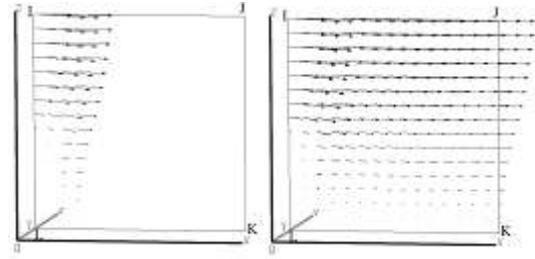
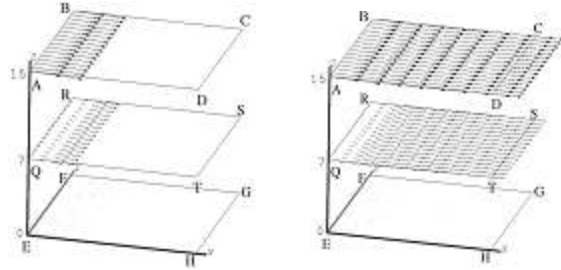


Fig. 7 case 3: Data are made lacking in shaded region which is 75% of all data.



(a)Initial flow (b)converged flow  
(A)vertical plane



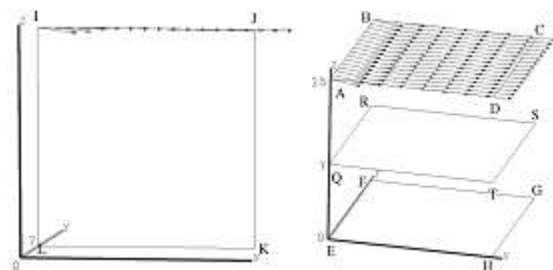
(a)Initial flow (b)converged flow  
(B)horizontal plane

Fig. 8 Recovered flow of Fig.7(case 3).

We calculated the numerical evaluations of the proposed method by mean square error(NRMSE) shown Eq.(14). The velocity field of the lack-place can be reconstructed for almost all cases.

**C. 3D optical flow from top surface image data**

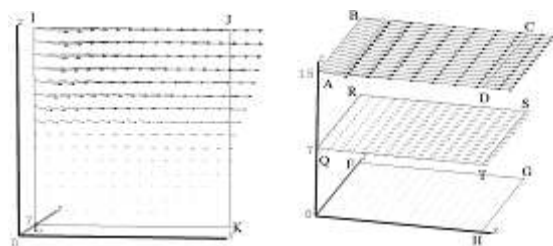
As the simulation of section 5.B, we intentionally made short cut of data and estimated the lacking data using our method, where the data were recovered by extrapolation and interpolation. it is valuable to estimate the 3D optical flow from top image data and a priori knowledge of the flow configuration.



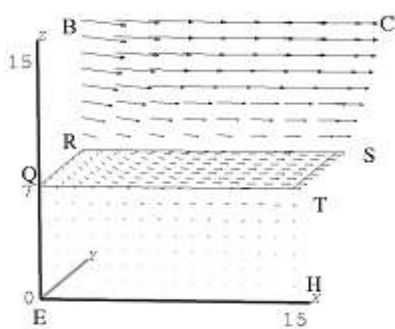
(a)vertical plane (b)horizontal plane

Fig. 9 Initial data for 3D flow.

[case 4] The 3D top surface image is easily obtained by noncontact way in practice. Initial value is shown in Fig. 9(a)(b). Optical flow obtained are shown in Fig. 10(a)(b)(c).



(a)vertical plane (b)horizontal plane



(c)oblique 3D optical flow

Fig. 10 3D flow (case 4).

The NRMSE given by Eq. (14) of 3D flow are shown in Table 1.

$$NRMSE = \frac{\sqrt{\sum \sum \sum ((u_{ijk}^t - u_{ijk}^c)^2 + (v_{ijk}^t - v_{ijk}^c)^2 + (w_{ijk}^t - w_{ijk}^c)^2)}}{\sqrt{\sum \sum \sum (u_{ijk}^t{}^2 + v_{ijk}^t{}^2 + w_{ijk}^t{}^2)}} \tag{14}$$

where  $u_{ijk}^t, v_{ijk}^t, w_{ijk}^t$  are true velocity of X, Y, Z component and  $u_{ijk}^c, v_{ijk}^c, w_{ijk}^c$  are calculated velocity of X, Y, Z component, respectively. It is very difficult to obtain the 3D optical flow by conventional algorithm. In our method, the 3D velocity field can be reconstructed as a whole. However, the lower part of the RQST plane are calculated in small values.

Table 1 Normalized error

Simulation case number	Number of iterations	NRMSE	
		Initial value	converged value
1	10000	0.352	0.077
2	4000	0.247	0.032
3	10000	0.861	0.114
4	20000	0.902	0.270

### VI. CONCLUSIONS

We proposed a method of using physics-based knowledge of the fluid motion. Here, we implemented it for the 3D fluid flow reconstruction of stream images using NSE. As a simulation, first, we intentionally made the artificial steady-flow with short of data and estimated the lacking data. As a result, almost all cases of the velocity field of the lack-place can be reconstructed. Next, we calculated the 3D flow by using practically usable surface image of the flow and a priori knowledge of flow construction. We evaluated the results by NMSE. Though 3D flow are obtained well, some parts are not so accurate. That is the problem remained to be solved.

### ACKNOWLEDGMENT

This work was supported by Kyungsung University Foundation Grant in 2008.

### REFERENCES

- [1] T. Kida, H. Ueda, and M. Kurata, "Pressure distribution of transient flow around an impulsively started two-dimensional elliptic cylinder by a vortex method," *CFD Journal*, vol. 9, pp. 64–75, July 2000.
- [2] J. -J. Hwang, and D. -Y. Lai, "Three-Dimensional Laminar Flow in a Rotating Multiple-Pass Square Channel With Sharp 180-Deg Turns," *CASME J. Fluids Eng.*, vol. 120, pp. 488–495, 1998.
- [3] Y. M. Chung, P. G. Tucker, and D. Roychowdhury, "Unsteady laminar flow and convective heat transfer in a sharp 180° bend," *International Journal of Heat and Fluid Flow*, vol. 24, pp. 67–76, 2003.
- [4] J. H. Sun, D. A. Yates, and D. E. Winterbone, "Measurement of the flow field in a diesel engine combustion chamber after combustion by cross-correlation of high-speed photographs," *Experiments in Fluids*, vol. 20, pp. 335–345, 1996.

- [5] B. K. P. Horn, and B. G. Schunck, "Determining optical flow," *Artificial Intelligence*, vol. 17, pp. 185–204, 1981.
- [6] B. K. P. Horn, "Robot Vision," *MIT Press*, Cambridge, Massachusetts, 1986.
- [7] D. Metaxas, and D. Terzopoulos, "Shape and nonrigid motion estimation through physics-based synthesis," *IEEE Trans. Patt. Anal. Machine Intell.*, vol. 15, pp. 580–591, June 1993.
- [8] D. Terzopoulos, and K. Waters, "Analysis and Synthesis of Facial Image Sequences Using Physical and Anatomical Models," *IEEE Trans. Patt. Anal. Machine Intell.*, vol. 15, pp. 569–579, June 1993.



**Kim, Jin Woo**

He received the B.S degree in Electrical Engineering from Myongji University in 1992 and the M.S and Ph.D. degrees in Electronic Engineering and System design Engineering from Fukui University, Fukui, Japan, in 1996 and 1999, respectively. From 2000 to 2003, he was a contract Professor in the Department of Information Communication and Computer Engineering at Hanbat National University, Daejeon, Korea. Since 2003 he has been with the Department of Multimedia and Communication Engineering at Kyungsung University, Busan, Korea, where he is currently an associate professor. From Dec., 2007 to Mar., 2009, he was a visiting researcher in the Department of Bioengineering at Tokyo University, Japan. His current research interests include image processing, pattern recognition, and medical imaging technology.